

Supplementary Materials for

The role of electron irradiation history in liquid cell transmission electron microscopy

Trevor H. Moser, Hardeep Mehta, Chiwoo Park, Ryan T. Kelly, Tolou Shokuhfar, James E. Evans

Published 20 April 2018, *Sci. Adv.* **4**, eaq1202 (2018)

DOI: 10.1126/sciadv.aq1202

The PDF file includes:

- fig. S1. Multiwindow chips compatible with commercial LC-TEM holders.
- fig. S2. Additional experimental data from Fig. 2.
- fig. S3. Imaging path and thickness of multiwindow devices for no flow versus flow.
- fig. S4. Low-dose imaging of biological samples.
- fig. S5. Improved sampling of nonuniform samples with multiwindow areas.
- fig. S6. Illustration of microfabrication workflow.
- Supplementary protocol for fabrication of multiwindow devices
- Legend for movie S1

Other Supplementary Material for this manuscript includes the following:

(available at advances.sciencemag.org/cgi/content/full/4/4/eaq1202/DC1)

- movie S1 (.mp4 format). Demonstration of in situ liquid cell “low-dose” imaging.

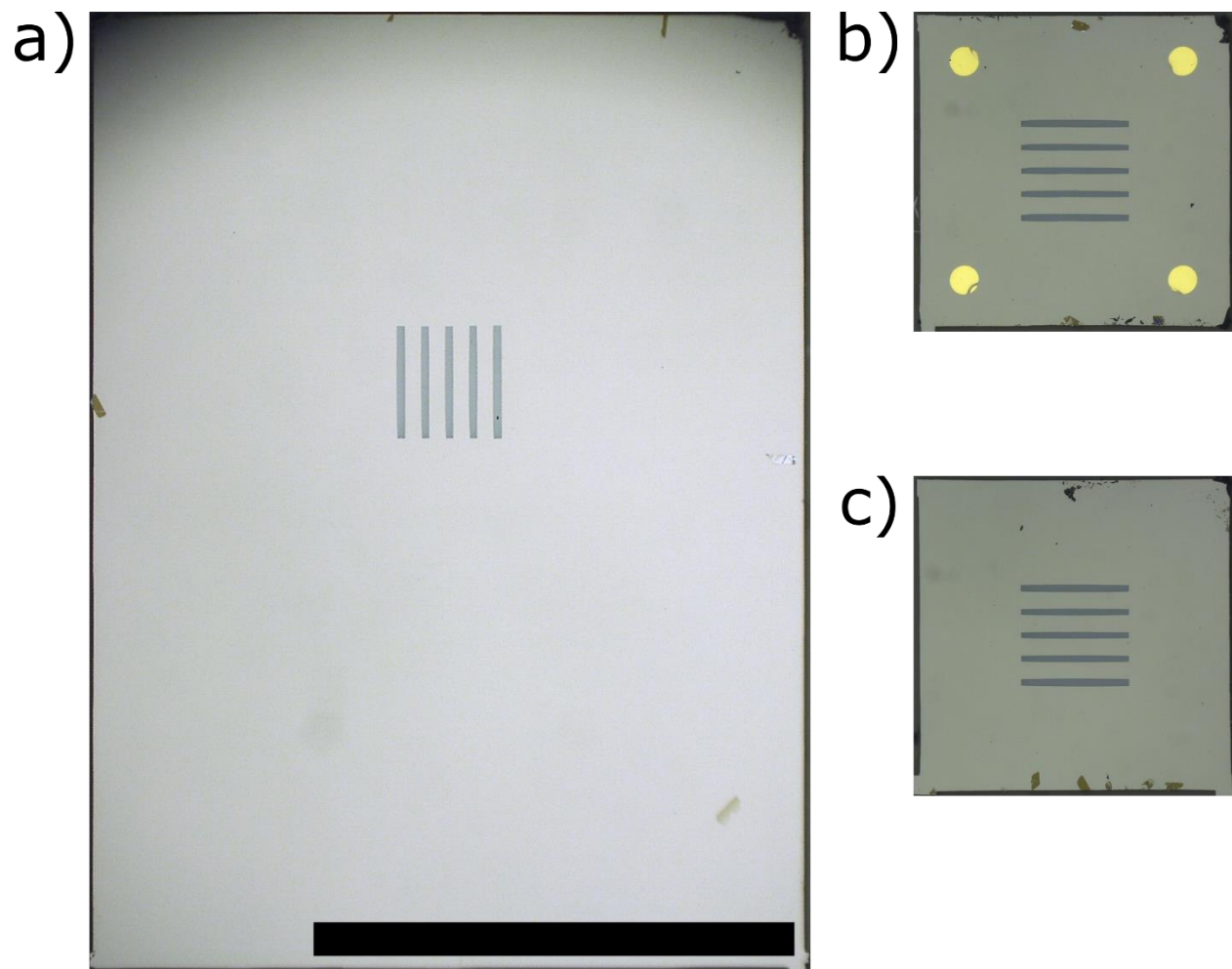


fig. S1. Multiwindow chips compatible with commercial LC-TEM holders. (A) Optical image of a multi-window nanofluidic device designed to fit the upper device of a commercial Protochips Liquid Stage holder. (B&C) Optical image of a multi-window nanofluidic device designed to fit the lower device of a commercial Protochips Liquid Stage holder with (B) and without (C) patterned Au spacer posts. Black scale bar in (A) represents 3mm and is equivalent for all images.

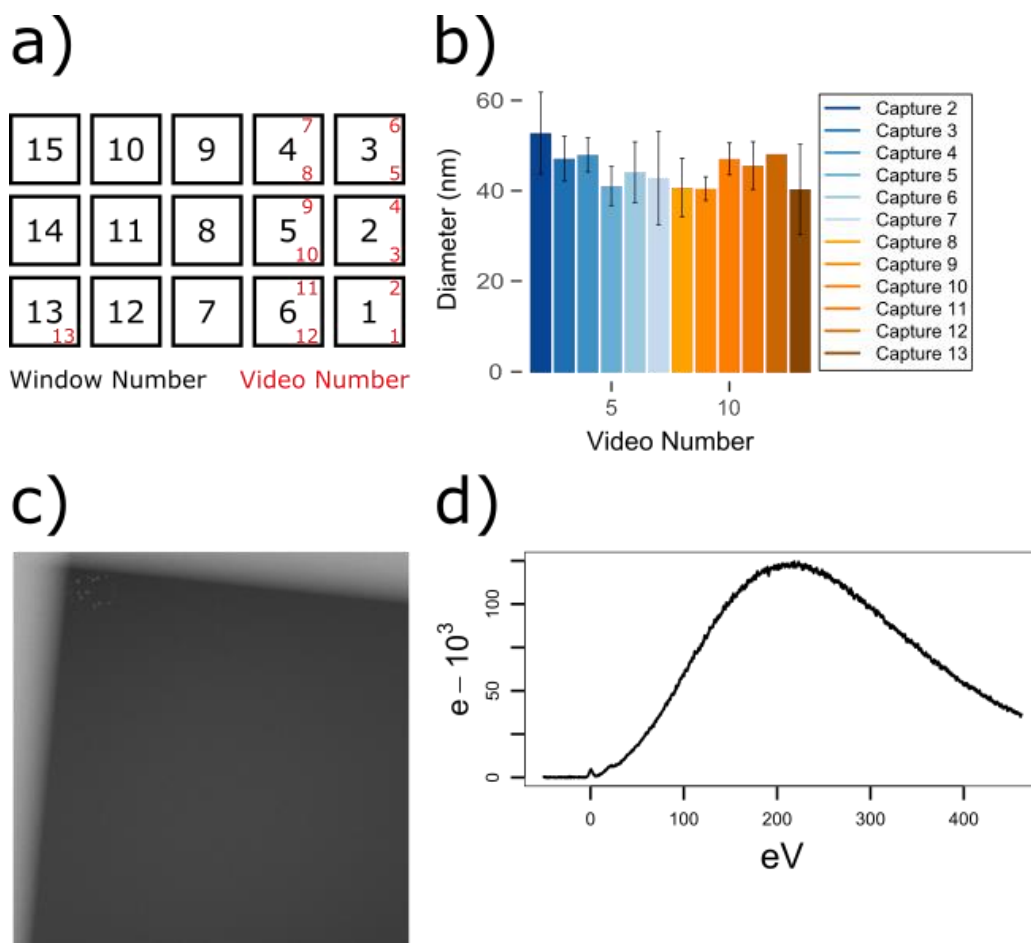


fig. S2. Additional experimental data from Fig. 2. (A) Layout of imaged windows (black numbers) and video acquisition location (red numbers) within the liquid cell corresponding to experiment highlighted in **Figure 2a-c**. (B) Mean final diameter of particles in each capture area after 200 STEM scans of electron irradiation/growth. (C) Low mag STEM scan of one of the corners for a video capture showing the characteristic contrast gradient from the corner to the center of the window commonly observed in hydrated LC-TEM samples. (D) EELS spectrum from (C) showing the thickness of the sample as evidence of hydration. Due to the small size of the zero-loss peak (ZLP), the spectra could not be quantified precisely but is >5 IMFP.

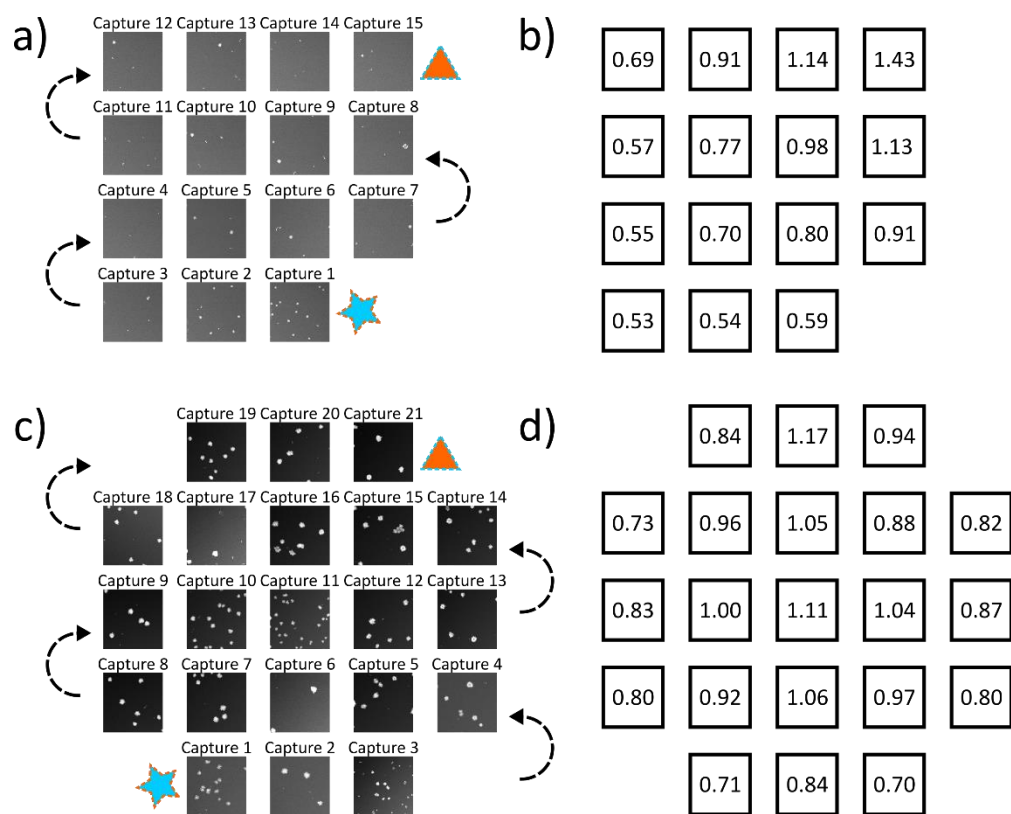


fig. S3. Imaging path and thickness of multiwindow devices for no flow versus flow. (A) Final frame of each video acquired from the data shown in **Figure 2d** where each capture represents the window position and order that the video was acquired in. Sample was 0.1mM AgNO₃ and not flowed during the course of the experiment. Each successive video was performed in an adjacent window for 200 STEM scans. The electron flux was 0.51 e⁻/Å² per scan and 101.4 e⁻/Å² per video. The blue star denotes the first video capture, while the orange triangle denotes the final video capture. Arrows denote the direction that sequential videos were acquired in successive windows. **(B)** IMFP measurements of each window corresponding to (A) where the mean thickness was 0.816 ± 0.266 IMFP. **(C)** Final frame of each videos acquired from the data shown in **Figure 2e** where each image represents the window position that the video was acquired in. Sample was 0.1mM AgNO₃ and solution is flowed at a rate of 0.5µL/min during the course of the experiment. Each successive video was performed in an adjacent window for 200 STEM scans. The electron flux was the same as in (A) and both the first video capture (blue star) and final video capture (orange triangle) are indicated. **(D)** IMFP measurements of each window corresponding to (C) where the mean thickness was 0.906 ± 0.132 IMFP.

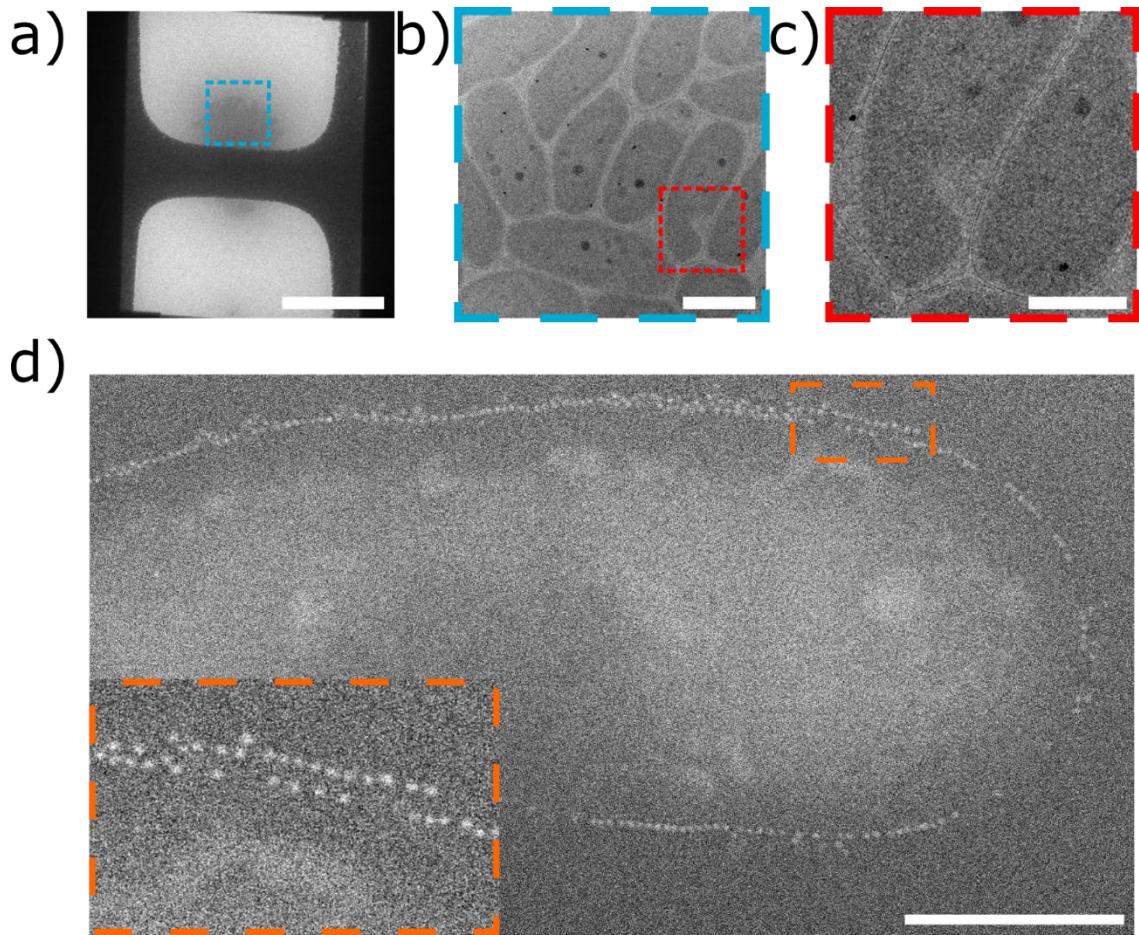


fig. S4. Low-dose imaging of biological samples. (A) Low magnification image of *Cupriavidus metallidurans* cells in an assembled nanofluidic device with patterned grid bars for use as low-dose focusing aids. (B) Higher mag image of cells from (A) taken with minimal electron flux prior to acquisition. Cumulative dose of image was $0.5 \text{ e}^-/\text{\AA}^2$. (C) Enlarged section of (B) highlighting cell membranes and other subcellular features visible due to low-dose focusing and image capture. (D) STEM HAADF image of a bacteria with 10nm Au nanoparticles surrounding the outside of the cell. Inset shows enlarged region around cell and individual nanoparticles. Scale bars in (A)-(D) are $10\mu\text{m}$, $1\mu\text{m}$, 500nm , and 500nm respectively.

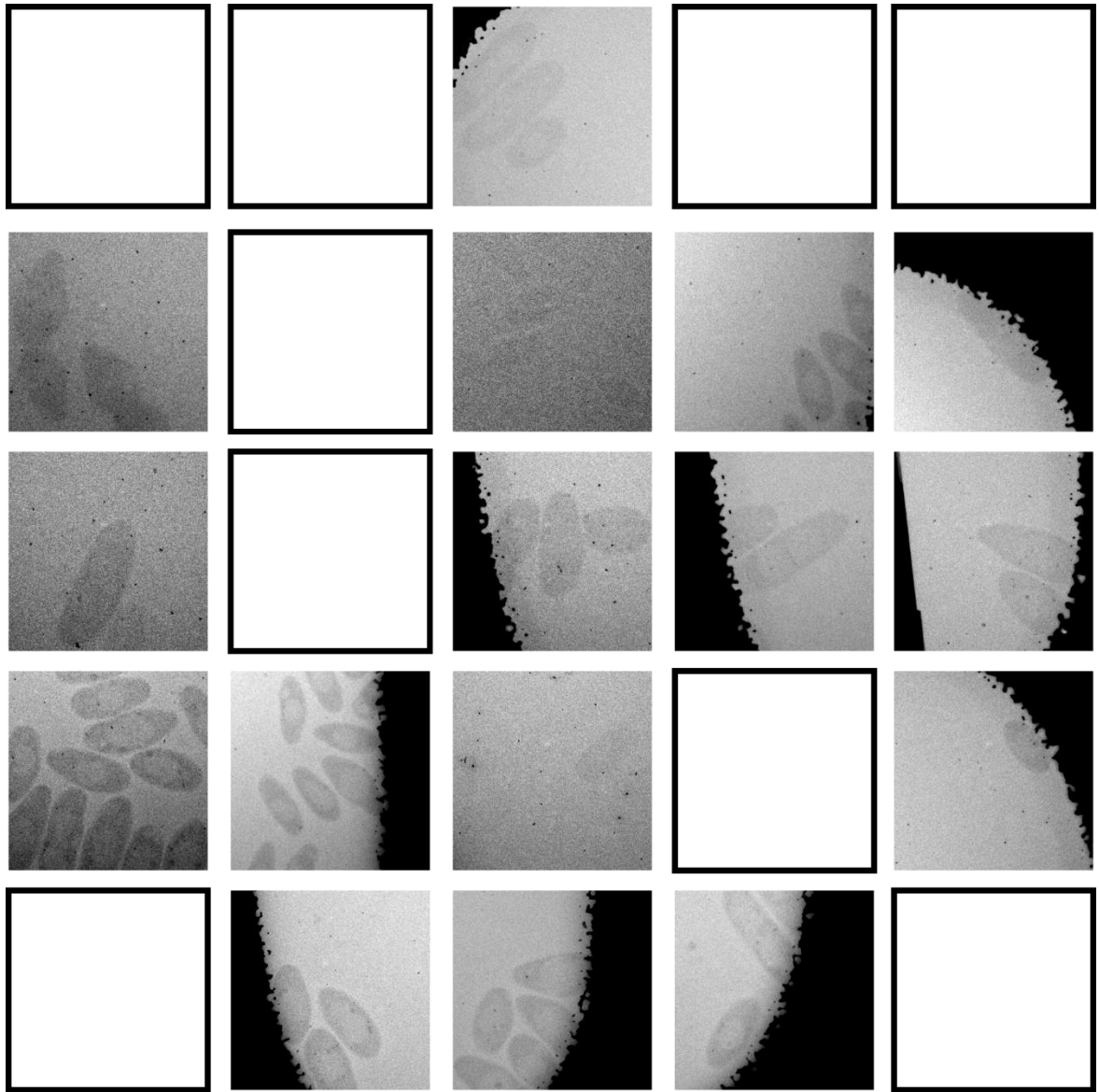


fig. S5. Improved sampling of nonuniform samples with multiwindow areas. Tiling of bright field LC-TEM images of *C. metallidurans* taken from a single device with a 5x5 array of windows for a total number of 25 imaging regions. Images depict the corresponding windows in the array if at least 1 cell was detected in the region. Window regions with no cells present in the visible window are left blank. In total, cells were found in 16 of the 25 possible imaging areas for this singular device. Distance between windows is not to scale but is $\sim 100\mu\text{m}$ and the window area is $\sim 40\mu\text{m} \times 40\mu\text{m}$.

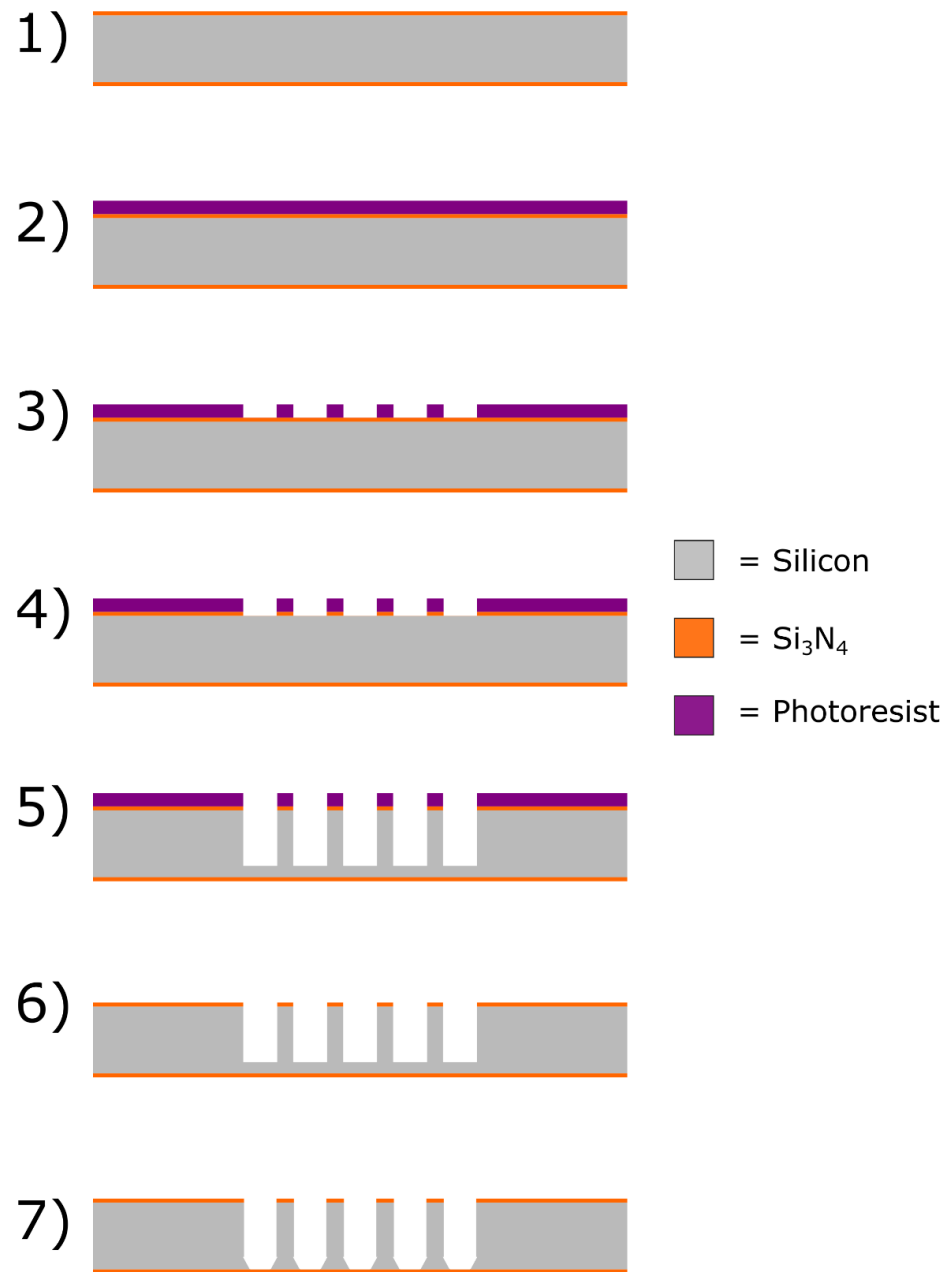


fig. S6. Illustration of microfabrication workflow. Schematic of wafer viewed from the side for patterning, etching, and window formation steps during microfabrication of multi-window devices.

Supplementary protocol for fabrication of multiwindow devices

Standard processing steps for fabrication of the freestanding silicon nitride membranes of currently available nanofluidic devices typically entail a wet etch of the silicon substrate with concentrated potassium hydroxide (KOH). Silicon nitride patterned on both sides of the wafer is used both to define the etching region as well as acting as an etch stop for forming the final membrane. The resistance of silicon nitride to KOH allows for precise control over final membrane thickness, where the thickness of silicon nitride deposited on the wafer is ultimately the thickness of the free-standing membrane, typically 10-50nm. While advantageous for creating the very thin membranes needed for TEM imaging, the well characterized anisotropic etch geometry of silicon by KOH along the (111) plane results in inward tapering pits, where the required starting etch area is much larger than the resulting free-standing membrane. When KOH etching is used to etch the silicon substrate and form the freestanding membrane, the resulting requirement for initial etching surface area to produce a window $\sim 50\mu\text{m}$ in width constrains the number of windows on commercially compatible devices to one.

Maximizing available equivalent imaging area was accomplished by creating multiple free-standing membranes per device. The limitation of the KOH etch profile described above was overcome via microfabrication mask redesign and process optimization to reduce the effective etching region area on the backside of the device. This was accomplished by performing the majority of the through wafer etching with a Bosch etch, which results in a high aspect ratio etch profile with nearly vertical sidewalls as opposed to the sloped etch profile of KOH. After etching $\sim 90\text{-}95\%$ of the wafer thickness with this process, the final $\sim 5\text{-}10\%$ was etched using the conventional KOH wet etch for membrane formation to compensate for the non-selectivity of the Bosch process etch with silicon nitride. While this resulted in tapering of the sidewalls over the final distance of etching, the decreased wet etch duration allowed for significantly smaller starting etch profiles and allowed for five rectangular windows to be fit on a single device without compromising the required sealing area of the o-ring for commercial holders. When assembled and loaded with one device rotated 90-degrees with respect to the other, a 5x5 array of available imaging windows is created. The detailed fabrication process to achieve this geometry is as follows:

Wafers were first patterned with gold spacer and grid bars.

1. Wafers spin coated with AZ 5214E (MicroChemicals) at 3000rpm for 60s, followed by a soft bake at 90C for 2 min.
2. Resist exposed for 1.9s in an NXQ Q4000-6 mask aligner (Neutronix Quintel) with mask for grid bars.
3. Reverse baked for 2 min at 120C to create negative profile.
4. Flood exposure of entire wafer for 30s in mask aligner.
5. Developed in 100mL fresh AZ350 (MicroChemicals) at a ratio of AZ350:Water (1:5).
6. Loaded into a Discovery Sputter System 785 (Denton Vacuum) with Cr and Au targets purchased from Kurt Lesker.
 - a. Chromium deposited at 50W for 50s and 10mtorr argon (~10nm thickness)
 - b. Au deposited at 50W for 200s and 10mtorr argon (~100nm thickness)
7. Wafers transferred to acetone bath with sonication for lift off, leaving behind grid bars.

Steps 1-7 were then repeated for spacer post patterning, with front side alignment of spacer posts to the grid bar features and an Au deposition time of 600s resulting in spacer posts 300nm in height. Wafers were then prepared for membrane etching.

8. On backside of wafer (opposite side from grid bars and spacer posts) hexamethyldisilazane (HDMS) (Sigma Aldrich) spin coated at 3000rpm for 30s and allowed to dry.
9. AZP4620 (MicroChemicals) spin coated on same side at 1500rpm.
10. Resist soft baked for 3 min at 70C and 4 min at 110C followed by rehydration at room temperature for 30 min.
11. Backside alignment was used to align window mask with grid bars and spacer posts and resist was exposed for 20s.
12. Resist developed in ~100mL fresh AZ400K (MicroChemicals) at a ratio of AZ400K:Water (1:3) and hard baked at 180C for 30 min.

After hard bake, wafers were etched using a Plasmalab System 100 (Oxford Instruments) with a DRIE Bosch etch recipe. Because DRIE can be slightly variable wafer to wafer, the etching was performed gradually while measuring the depth of etching with an Zygo Optical Profilometer NewView 200 (Zygo) between each DRIE run in order to avoid over etching through the wafer. Typically for the instrument used, etching was performed as follows:

13. 240 Bosch Cycles, depth measured to be $\sim 100\mu\text{m}$
14. 150 Bosch Cycles, depth measured to be $\sim 165\mu\text{m}$
15. 40 Bosch Cycles, depth measured to be $\sim 180\mu\text{m}$
16. 20 Bosch Cycles, depth measured to be $\sim 190\mu\text{m}$

Generally, the number of cycles run was adjusted as needed based on the measured depth of the etching in order to reach a final depth of $\sim 190\mu\text{m}$. The remaining resist was stripped with Nanostrip 2x (KMG Electronic Chemicals) at 110C, and the remaining $10\mu\text{m}$ of silicon was etched with 40% (w/v) KOH (Sigma Aldrich) at 80C for approximately 30 minutes. Etching is noted by the evolution of hydrogen gas, a result of the reaction between KOH and silicon. The wafer was monitored closely, as the etch completion becomes apparent when free standing windows are clearly seen when shining a light through the backside of the wafer. Over etching is a possible risk here, as the (111) planes of silicon continue to etch, although slowly, and wafers should not be left to etch longer than necessary. Upon completion, the wafer is removed from the KOH bath and rinsed 5x times with DI H₂O in order to remove excess KOH. Care should be used at this time as wafers are very fragile due to the patterned edge sectioning of the devices. Individual devices are broken free from the wafer easily with a pair of carbon tipped tweezers.

movie S1. Demonstration of in situ liquid cell “low-dose” imaging. Patterned Au grid bars provide high-contrast features within the viewing area for liquid cell experiments to permit a "low-dose" imaging scheme and control irradiance history. Using this approach, a pristine liquid cell image of 10nm diameter gold nanoparticles in solution is captured already at proper focus and with minimal prior electron flux.